Supporting Information

A Nickel-Based Coordination Compound with Tunable Morphology for High-Performance Anode and the Lithium Storage Mechanism

Yifei Lu †, Lei Wang †, Zhenzhu Lou †, Leilei Wang, Yi Zhao, Weiwei Sun, Li-Ping Lv, Yong Wang and Shuangqiang Chen *

Department of Chemical Engineering, School of Environmental and Chemical Engineering, Shanghai University, Shangda Road 99, Shanghai 200444, China; lyf19722737@shu.edu.cn (Y.L.); wang-lei@shu.edu.cn (Lei Wang); 2510775784@shu.edu.cn (Z.L.); 22722788@shu.edu.cn (Leilei Wang); zhaoyi@shu.edu.cn (Y.Z.); vivisun@shu.edu.cn (W.S.); liping_lv@shu.edu.cn (L.L.); yongwang@shu.edu.cn (Y.W.)

* Correspondence: chensq@shu.edu.cn; Tel.: +86-21-66136598

† These authors contributed equally to this work.

This WORD file includes:

Figures S1 to S8

Tables S1 to S2

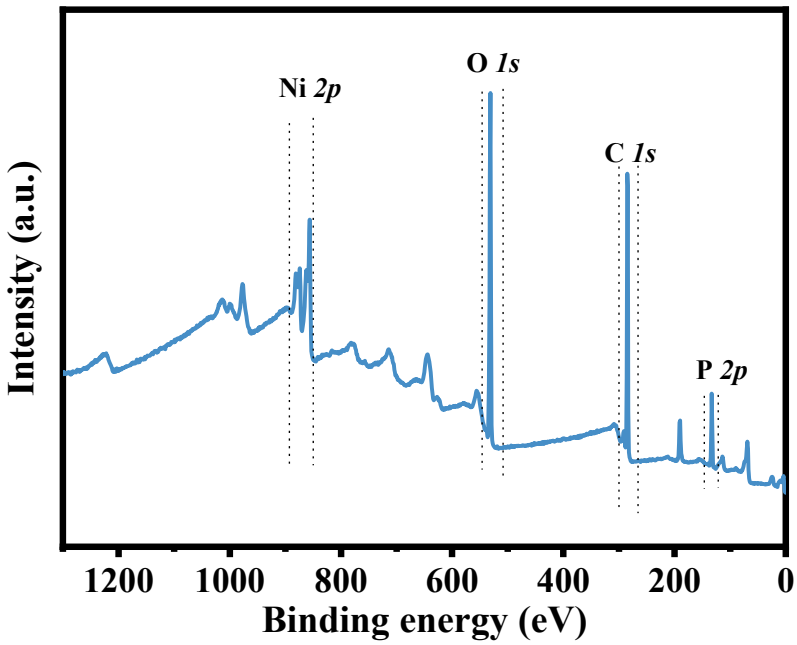


Figure S1. The survey spectrum of Ni-PP-2.

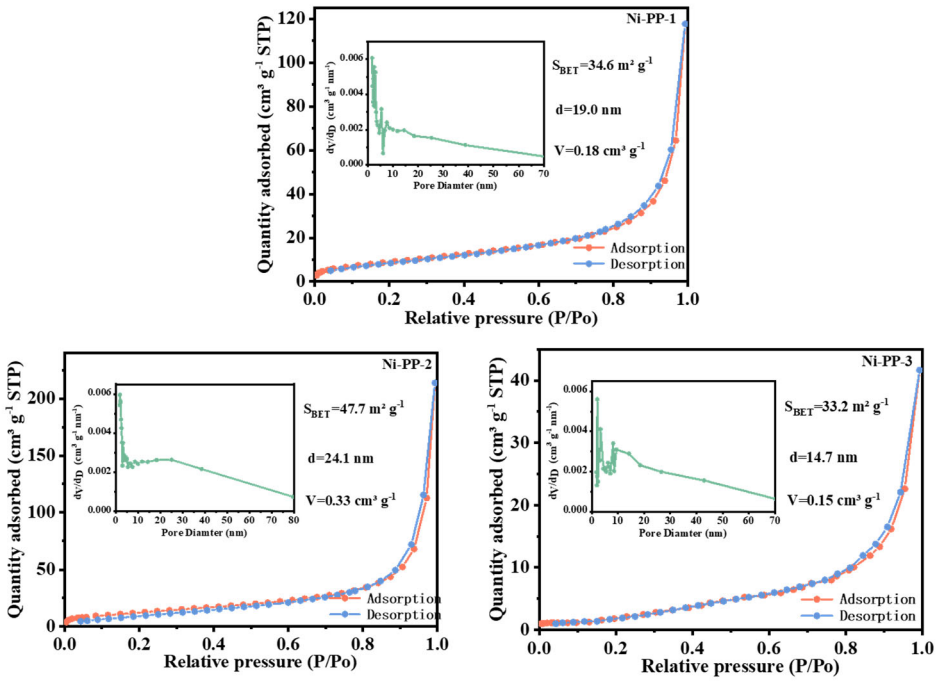


Figure S2. N_2 adsorption-desorption isotherms and pore size distribution of (a) Ni-PP-1, (b) Ni-PP-2, and (c) Ni-PP-3.

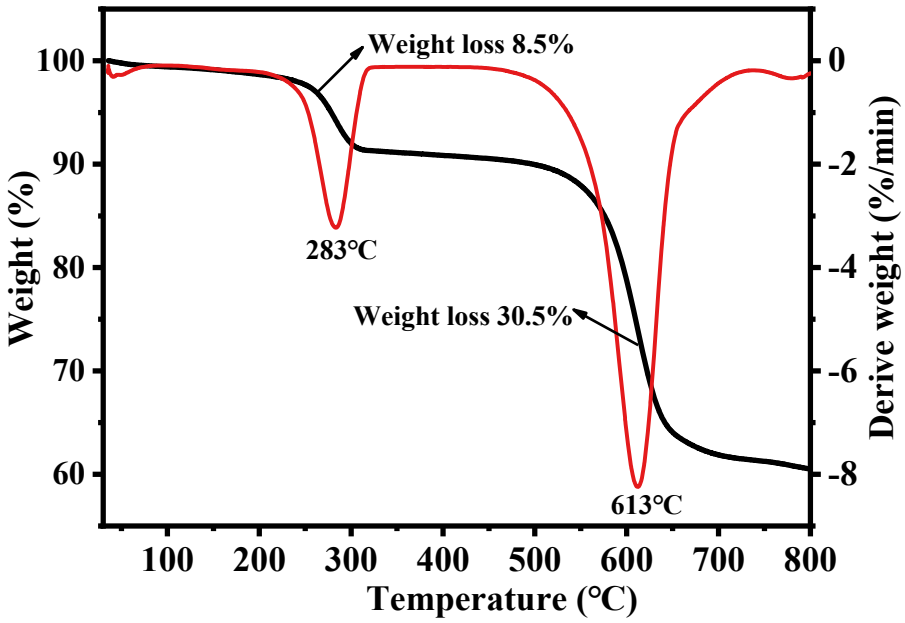


Figure S3. TG-DSC curves of Ni-PP-2.

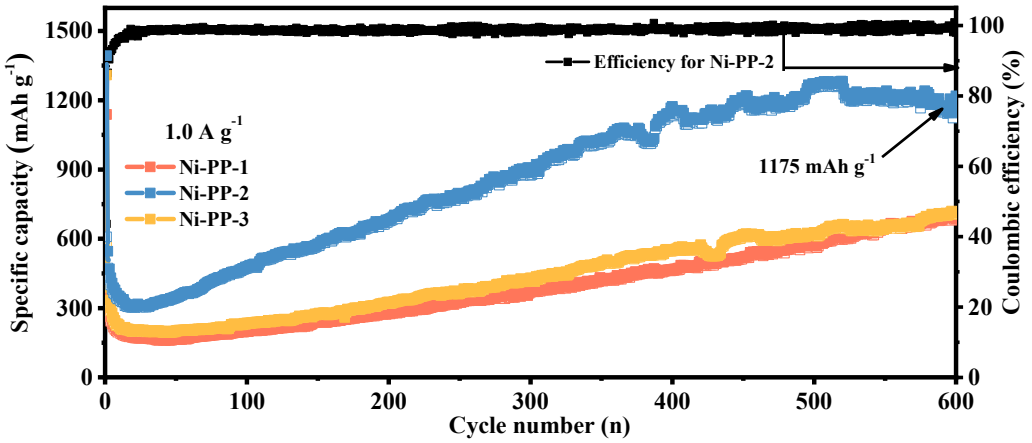


Figure S4. Cycling performances of Ni-PP-x (x = 1, 2, 3) at 1.0 A g^{-1}.

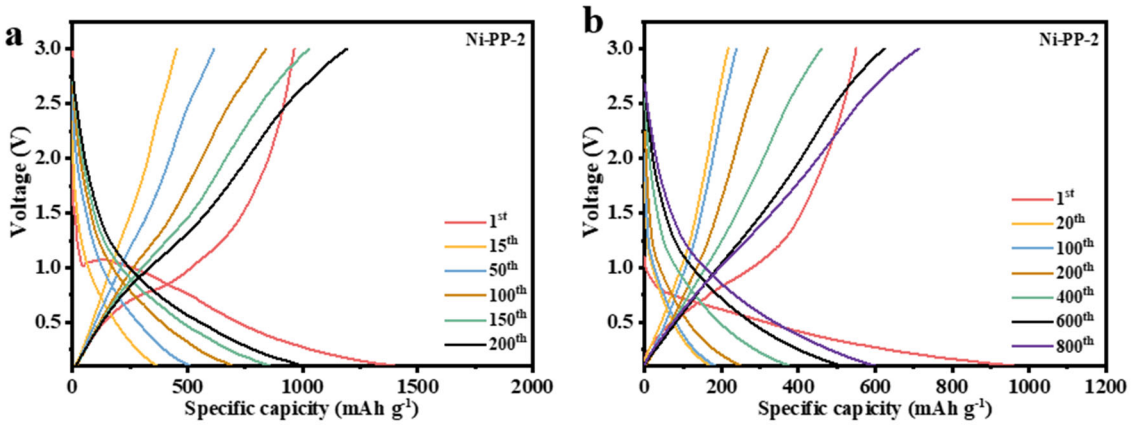


Figure S5. Charge/discharge curves of Ni-PP-2 at different cycles under (a) 0.2 A g^{-1}, and (b) 2.0 A g^{-1}.

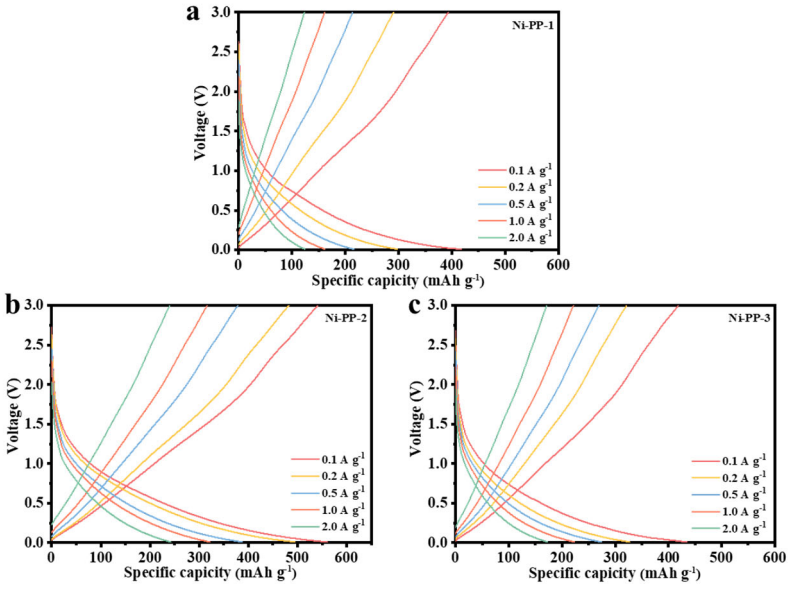


Figure S6. Charge/discharge curves of (a) Ni-PP-1, (b) Ni-PP-2, and (c) Ni-PP-3 at different current densities.

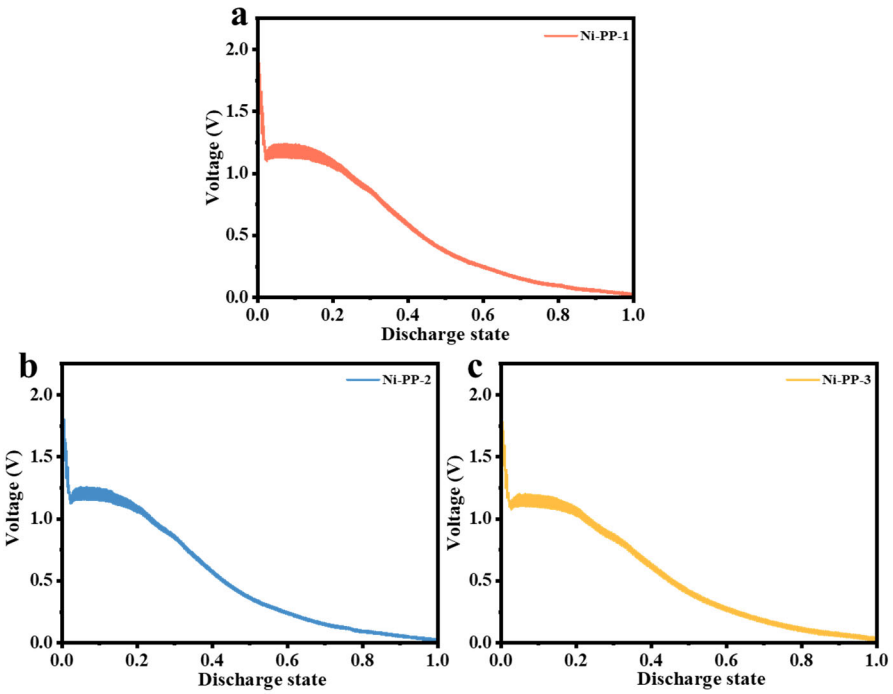


Figure S7. Initial discharge GITT curves of (a) Ni-PP-1, (b) Ni-PP-2, and (c) Ni-PP-3.

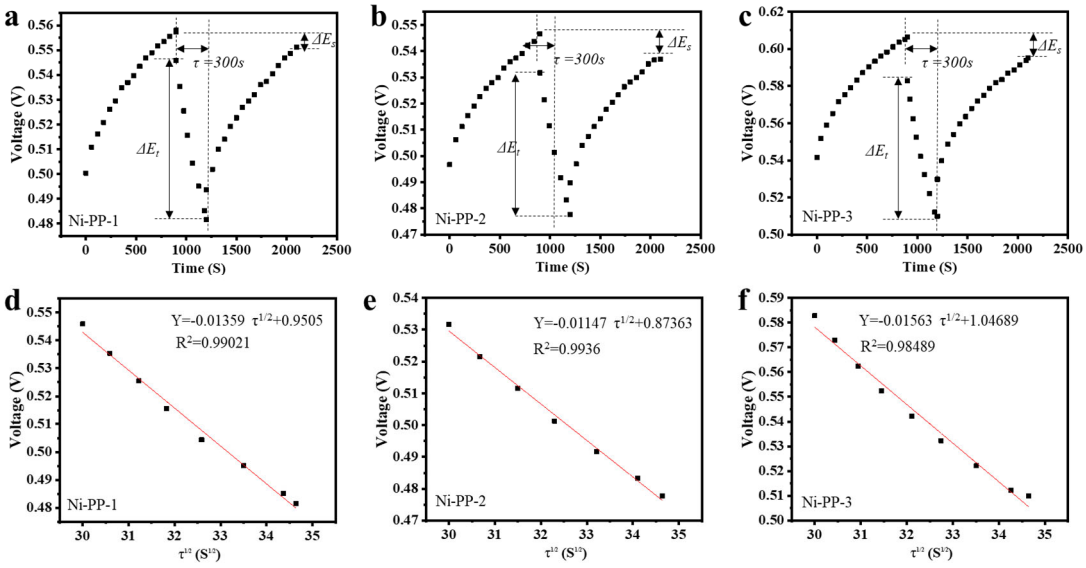


Figure S8. One single GITT profile of Ni-PP in the discharge process of (a) Ni-PP-1, (b) Ni-PP-2, and (c) Ni-PP-3. The corresponding linear relationship for the E versus $\tau^{1/2}$ in the discharge process of (d) Ni-PP-1, (e) Ni-PP-2, and (f) Ni-PP-3.

Table S1. Electrochemical performance of coordination compounds as anodes for LIBs. (RRC: retained reversible capacity, CD: current density).

Composite	Organic ligands	Preparation method	RRC [mAh g^{-1}]/ CD [A g^{-1}]	Cycle number	Ref.
Ni-PP-2	phenylphosphonic acid	Microwave assisted solvothermal	713/2	800	**This work**
H8L-Fe-MOF	(ethene-1,1,2,2-tetrayltetrakis(benzene-4,1diyl))tetraphosphonic acid	hydrothermal	275/0.05	50	[7]
Ni-MOF	4,4'-bpy	hydrothermal	49.2 /0.05	100	[8]
Ni–Me4bpz	3,3',5,5'-tetramethyl4,40-bipyrazole	hydrothermal	120/0.05	100	[9]
Ni-CAT	2,3,6,7,10,11-hexahydroxytriphenylene	hydrothermal	592/0.5	200	[10]
BP/NiCo MOF	benzenedicarboxylic acid	sonicated	596/2	250	[11]
Ni-NHM	2,3,6,7,10,11-hexaaminotriphenylene hexahydrochloric	hydrothermal	400/1	800	[12]
Ni-NDC	dicarboxylic acid	hydrothermal	310/1	500	[13]

Table S2. Fitting results of electrochemical impedance spectrum.

Composite	R1	R2	CPE1-T	CPE1-P	Wo-R	Wo-T	Wo-P
Ni-PP-1 (Pristine)	7.32	224.0	4.27×10^{-5}	0.72	64.68	0.025	0.47
Ni-PP-2 (Pristine)	0.96	151.6	1.91×10^{-5}	0.74	62.61	0.037	0.43
Ni-PP-3 (Pristine)	2.89	213.7	5.5×10^{-5}	0.67	35.70	0.016	0.44
Ni-PP-1 (100^{th} cycle)	21.48	142.8	4.84×10^{-5}	0.69	34.22	0.029	0.28
Ni-PP-2 (100^{th} cycle)	22.30	99.5	6.17×10^{-5}	0.70	24.92	0.027	0.34

Ni-PP-3 (100th cycle)	18.38	123.0	6.09×10^{-5}	0.70	36.57	0.042	0.31

References

1. Chakraborty, D.; Dam, T.; Modak, A.; Pant, K.K.; Chandra, B.K.; Majee, A.; Ghosh, A.; Bhaumik, A. A novel crystalline nanoporous iron phosphonate based metal-organic framework as an efficient anode material for lithium ion batteries. *New J. Chem.* **2021**, *45*, 15458-15468, doi:10.1039/d1nj02841c.
2. Chang, H.-L.; Bai, Y.-W.; Song, X.-Y.; Duan, Y.-F.; Sun, P.-P.; Tian, B.; Shi, G.; You, H.; Gao, J.; Shi, F.-N. Hydrothermal synthesis, structural elucidation and electrochemical properties of three nickel and cobalt based phosphonates as anode materials for lithium ion batteries. *Electrochim. Acta* **2019**, *321*, 134647, doi:10.1016/j.electacta.2019.134647.
3. An, T.; Wang, Y.; Tang, J.; Wang, Y.; Zhang, L.; Zheng, G. A flexible ligand-based wavy layered metal-organic framework for lithium-ion storage. *J. Colloid Interface Sci.* **2015**, *445*, 320-325, doi:10.1016/j.jcis.2015.01.012.
4. Guo, L.; Sun, J.; Sun, X.; Zhang, J.; Hou, L.; Yuan, C. Construction of 1D conductive Ni-MOF nanorods with fast Li^+ kinetic diffusion and stable high-rate capacities as an anode for lithium ion batteries. *Nanoscale Adv.* **2019**, *1*, 4688-4691, doi:10.1039/c9na00616h.
5. Jin, J.; Zheng, Y.; Huang, S.-z.; Sun, P.-p.; Srikanth, N.; Kong, L.B.; Yan, Q.; Zhou, K. Directly anchoring 2D NiCo metal-organic frameworks on few-layer black phosphorus for advanced lithium-ion batteries. *J. Mater. Chem. A* **2019**, *7*, 783-790, doi:10.1039/c8ta09327j.
6. Yueji Cai, W.W., Xuanxuan Cao, Lingfei Wei, Caichao Ye, Chunfeng Meng, Aihua Yuan,* Huan Pang,* and Chao Y. Synthesis of tostadas-shaped metal-organic frameworks for remitting capacity fading of Li-ion batteries. *Adv. Funct. Mater* **2022**, *32*, 1209927, doi:10.1002/adfm.202109927.
7. Shi, Y.; Zhu, G.; Guo, X.; Jing, Q.; Pang, H.; Zhang, Y. Three-dimensional MXene-encapsulated porous Ni-NDC nanosheets as anodes for enhanced lithium-ion batteries. *Nano Research* **2022**, *16*, 2528-2535, doi:10.1007/s12274-022-5168-7.